Ecosystems
https://doi.org/10.1007/s10021-023-00889-3

Six Decades of Changes in Pool Characteristics on a Concentric-Patterned Raised Bog

Daniel W. Colson,[1]* Paul J. Morris,[1] Mark W. Smith,[1] Håkan Rydin,[2] Gustaf Granath,[2] and Duncan J. Quincey[1]

[1]*School of Geography, University of Leeds, Leeds, UK;* [2]*Department of Ecology and Genetics, Evolutionary Biology Centre, Uppsala University, Uppsala, Sweden*

Abstract

Raised bogs are wetland ecosystems which, under the right climatic conditions, feature patterns of pool hollows and hummock ridges. The relative cover and the spatial arrangement of pool and ridge microforms are thought to be influential on peatland atmosphere carbon gas fluxes and plant biodiversity. The mechanisms responsible for the formation and maintenance of pools, and the stability of these features in response to warming climates, remain topics of ongoing research. We employed historical aerial imagery, combined with a contemporary uncrewed aerial vehicle survey, to study 61 years of changes in pools at a patterned raised bog in central Sweden. We used a pool inheritance method to track individual pools between image acquisition dates throughout the time series. These data show a rapid loss of open-water pool area during the study period, primarily due to overgrowth of open-water pools by *Sphagnum*. We postulate that these changes are driven by ongoing climate warming that is accelerating *Sphagnum* colonisation. Open-water pool area declined by 26.8% during the study period, equivalent to a loss of 1001 m^2 y^{-1} across the 150-hectare site. This is contradictory to an existing theory that states pools are highly stable, once formed, and can only convert to a terrestrial state through catastrophic drainage. The pool inheritance analysis shows that smaller pools are liable to become completely terrestrialised and expire. Our findings form part of a growing body of evidence for the loss of open-water habitats in peatlands across the boreal and elsewhere.

Key words: Concentric bog; Peatland; Infilling; Pool dynamics; Remote sensing; *Sphagnum*.

Highlights

- 61 years of changes reveal a decrease in open-water pool areas.
- Pool inheritance methodology used to track individual pool changes through time.
- Loss of open-water pool area driven by vegetation encroachment and pool infilling.

Received 27 July 2023; accepted 13 November 2023

Supplementary Information: The online version contains supplementary material available at https://doi.org/10.1007/s10021-023-00889-3.

Author Contributions D.W.C., P.J.M., M.W.S. and D.J.Q. conceived and designed the study. D.W.C., P.J.M., M.W.S., H.R. and G.G. conducted the fieldwork. D.W.C. analysed the data and led manuscript development, with contributions from all authors.

**Corresponding author; e-mail:* eedwc@leeds.ac.uk

Published online: 18 December 2023

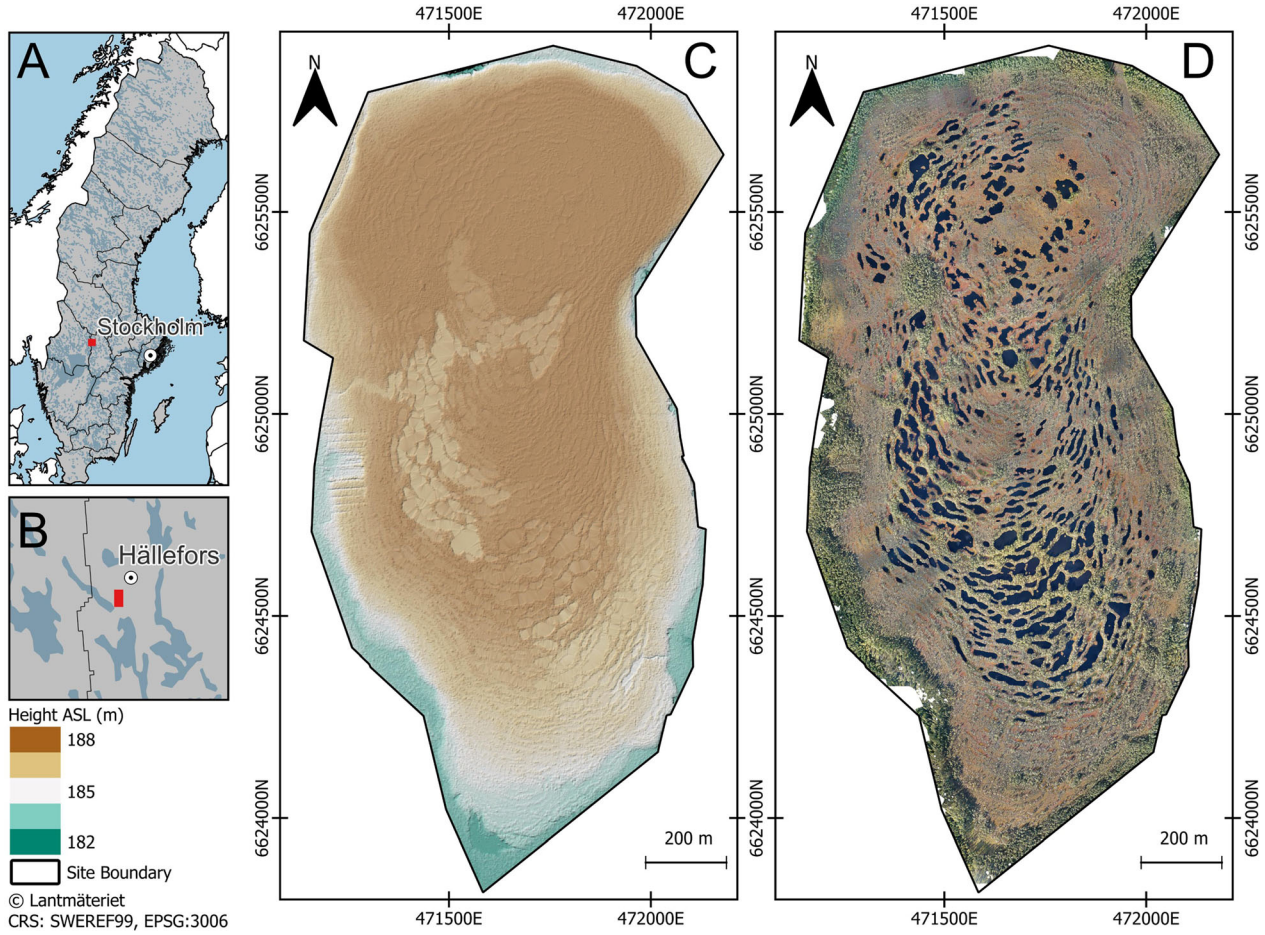

Figure 1. Location of Hammarmossen within Sweden (**A**, **B**) with Natura 2000 site boundary and details of (**C**) topography, derived from Lantmäteriet supplied LiDAR data, highlighting the domed nature of the site and (**D**) 2022 UAV orthomosaic.

Introduction

Peatlands are organic-rich wetland ecosystems, covering approximately 3% of the Earth's land surface (Xu and others 2018a). Northern peatlands (that is, those north of ~ 45°N) play an important role in the global carbon cycle (Gorham 1991; Page and others 2011; Loisel and others 2021), containing around 600 Gt of carbon (Gorham 1991; Müller and Joos 2020), equivalent to between a sixth and a third of all global soil carbon (Page and others 2011; Scharlemann and others 2014). The majority of present-day northern peatlands have formed since the Last Glacial Maximum (~ 21,000 years before present), driven by deglacial climate change and ice sheet retreat (Ruppel and others 2013; Morris and others 2018; Müller and Joos 2021). Carbon is accumulated in the form of peat, largely as a result of the waterlogged and acid conditions created by the dominant peat-forming mosses (*Sphagnum*; Rydin and Jeglum 2013). Northern peatlands also offer a habitat for specialised fauna and flora (for example, Rydin and Jeglum 2013), and in some parts of the world also provide an important source of human drinking water (Xu and others 2018b).

Raised bogs are a type of peatland characterised by a gently convex-upward surface, meaning that they are local sources of runoff to the surrounding landscape, and receive water and nutrients solely from precipitation, a condition known as ombrotrophy. This reliance on atmospheric water means that raised bogs are commonly claimed to be particularly sensitive to climate change (Almquist-Jacobson and Foster 1995; Turner and others 2014; Magnan and others 2022). Raised bogs generally have a continuous *Sphagnum* cover, alongside shrubs, graminoids, sedges and forbs (Arsenault and others 2019; Steenvoorden and others 2022). Individual raised bog ecosystems often feature microtopographic mosaics of distinct vegetation communities. Distinct microforms include raised,

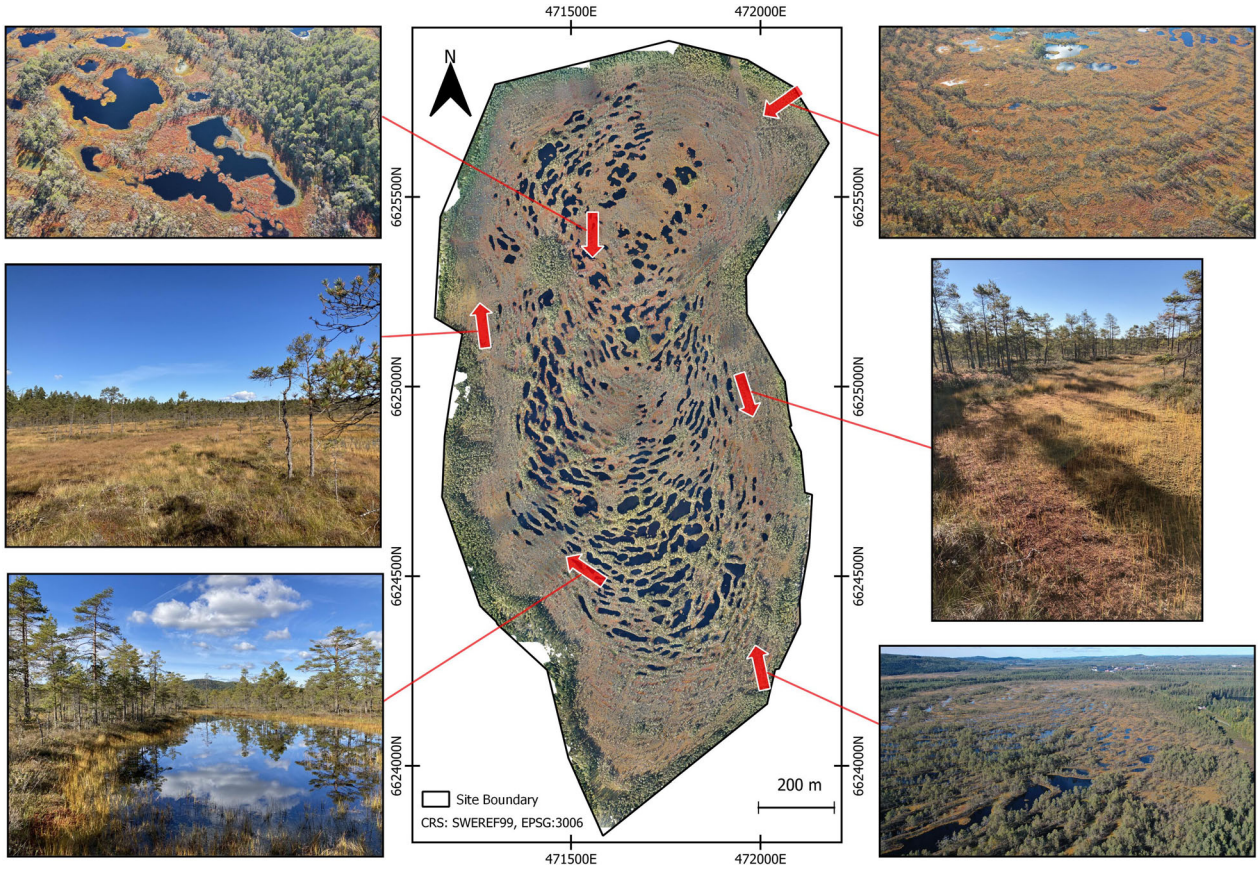

Figure 2. Contextual images showing peatland-scale details at time of UAV survey (left and right margins). Natura 2000 site boundary with UAV orthomosaic in centre panel. Red arrows in the centre panel indicate orientation of marginal photographs.

dry hummocks, hollows (firm lawns at intermediate level and soft, almost floating carpets) and open-water pools (Sjörs 1948; Foster and Wright 1990). Pools can be as deep as 3 or 4 m and comprise mainly an open-water body in which some detritus may be found (Foster and Wright 1990; Lindsay 2010; Beadle and others 2015). The sizes and spatial arrangements of these pools play an important role in determining carbon gas fluxes between peatlands and the atmosphere (Arsenault and others 2019; Chapman and others 2022).

In some peatlands, microhabitats are arranged into striking, non-random patterns, including concentric, semi-continuous rings of alternating strings of hummocks, hollows and pools, aligned semi-parallel with topographic contours (for example, Figure 1). The pools are thought to be secondary structures that develop some time after the formation of the bog (Foster and Fritz 1987), and a number of theories have been proposed to account for the development and maintenance of peatland pools, including in patterned sites. Foster and Wright (1990) hypothesised that vertical accretion of peat allows micro-scale topographic differences to develop. In turn, this causes water to collect in low-lying areas to form pools, with smaller pools coalescing and enlarging through bog development. Foster and Wright (1990) also proposed that, as a peatland expands laterally, older, central pools become deeper, while younger, shallower pools form towards the edge of the site. Belyea (2007) posited that once pools are formed and contain surface water throughout the year, reversal back to a terrestrial state becomes highly unlikely unless catastrophic drainage occurs (see also Belyea and Clymo 2001). Through different combinations of peat accretion, water ponding and nutrient accumulation interactions, the development of peatland surface patterns occurs (Eppinga and others 2009a). Theoretical studies indicate that water stress is the key regulator of stable and stationary mazing pattern distributions (Eppinga and others 2009a, 2009b). However, other landscape models indicate that patterning can move downslope, irrespective of underlying stresses (Swanson and Grigal 1988; Couwenberg and Joosten 2005),

with Pedrotti and others (2014) recording down slope movement of hummocks over a 50-year period in a field-based study.

Some recent studies have indicated that ongoing changes in climate and land use are causing northern peatlands to lose wet habitats such as pools and hollows, and that these are being replaced by drier microhabitats. Using testate amoeba-based reconstructions of paleohydrological conditions, Swindles and others (2019) found substantial drying in peatlands across Europe over the last 300 years, while Zhang and others (2022a) observed complex peatland ecohydrological dynamics in high-latitude peatlands over a similar time period, with 54% of sites becoming drier and 32% becoming wetter. Studies reporting direct observation of multi-decadal changes in pool structures are rare. Canadian-based studies have observed shifts to drier peatland ecosystems, linked in part due to substantial climatic warming with stable precipitation levels (Magnan and others 2018, 2022). At the scale of individual peatlands, reduction in open-water area has been observed at peatlands in Finland (Granlund and others 2022; Kolari and others 2022) and Ireland (Steenvoorden and others 2022). These changes have been attributed to warmer temperatures leading to prolonged growing seasons for *Sphagnum* in fen ecosystems (Granlund and others 2022; Kolari and others 2022; Steenvoorden and others 2022).

We sought to characterise multi-decadal changes in open-water pool area on a concentric-patterned, boreal raised bog in central Sweden, utilising new and existing high-resolution aerial imagery. As well as quantifying any variations in total pool area, we also sought to establish the nature of any fluctuations, which might shed light on the mechanisms and drivers of change.

Materials and Methods

Methodological Overview

We employed historical aerial photography in conjunction with uncrewed aerial vehicle (UAV) digital survey techniques to characterise changes in the areal coverage and spatial arrangement of open-water pools at a concentric-patterned raised bog in Sweden over a period of 61 years. We utilised remote sensing and GIS techniques in combination with a pool inheritance methodology to quantify spatiotemporal dynamics in open-water pools. Our study site, Hammarmossen, is the same one studied by Foster and Wright (1990), upon which their theories about long-term pool development and maintenance were developed.

Study Area

Hammarmossen is a large raised bog in Hällefors, Örebro County, central Sweden (Figure 1, 59° 45′ 46.89″ N, 14° 29′ 44.88″ E, 150 hectares, 185 m a.s.l.). Peatlands in this region typically originated by paludification of terrestrial ecosystems, as opposed to overgrowth of waterbodies (Foster and others 1988; Almquist-Jacobson and Foster 1995). Peat formation at Hammarmossen started ~ 6000 calendric years before present (cal. BP) across a broad glacial outwash plain of fine-to-medium sand that slopes gently to the south, with a marginal slope of 2.6% (Almendinger and Leete 1998). The fen spread laterally in all directions to the current extent shown in Figure 1 (Foster and Wright 1990; Loisel and others 2017). As detritus accrued and the surface became isolated from the poorly drained sand, the *Carex*-dominated fen developed into a *Sphagnum* bog, deriving nutrients and moisture from atmospheric sources (Foster and others 1988; Almquist-Jacobson 1994). The present-day site is characterised by extensive broad, concentric ridges and pools across two conjoined domes. The topographic highpoint is elevated ~ 6 m above the margin (Figure 1C) and is formed by a small rock outcrop covered by thin peat to the south-west of the northern dome. Open-water pools range from less than 2 m to more than 100 m in length and cover ~ 30% of the total peatland area (Sjörs 1948; Foster and Wright 1990; Loisel and others 2017). Foster and Wright (1990) surveyed the site and showed that the pools developed from 4200 to 1900 cal. BP, noting pool age and depth decreased from the centre of the site to the margin.

Hammarmossen has been protected as a Natura 2000 site (code SE0240036) since 1995, under the Birds Directive and Habitats Directive. Hollows surrounding the pools are characterised by carpets of *Sphagnum balticum*, *S. cuspidatum*, *S. majus* and *S. magellancicum*, interspersed with *Carex limosa*, *Drosera anglica*, *Rhynchospora alba*, *Scheuchzeria palustris* and *Vaccinium oxycoccos*. The bog ridges are dominated by *Sphagnum fuscum* and *S. rubellum* as substrates for *Drosera rotundifolia* and *Rubus chamaemorus*. Most of them have a dense cover of the dwarf shrubs *Calluna vulgaris* and *Empetrum nigrum*, with *Rhododendron tomentosum* and *Vaccinium uliginosum* where the pine cover is denser, such as in the wooded fringe of the bog (Figure 2). Due to the protection of the site, it is almost pristine

except for an electrical pylon already present in historical aerial photography captured in 1961, located in the northeast of the site. Under the Köppen-Geiger climate classification Örebro County is classified as having a humid continental climate (Peel and others 2007; Mantilla and others 2023). The annual average temperature is 5.4 °C, the average precipitation is 732 mm y^{-1} and the length of the vegetation period (consecutive period of at least six days, during which daily average temperature is above 5 °C) is 185 days per year (1961–2018 averaging period; Swedish Meteorological and Hydrological Institute (SMHI) 2022). We selected Hammarmossen as our study site due to (i) its accessibility, (ii) its strong concentric patterning, (iii) its close-to-pristine condition, (iv) its use in peatland theoretical work and (v) the availability of a long record of aerial photography (see below). Further information about the site can be found in Foster and Wright (1990).

Uncrewed Aerial Vehicle Survey

We visited the study site in September 2022 to conduct a very high-resolution UAV survey to illustrate present-day patterning and complement historical aerial images. In order to georeference UAV outputs precisely, we deployed 20 plastic Ground Control Points (GCPs, Figure S1) across the site, each of which consisted of a white cross against a black background. We located the central cross of each GCP using a Leica GS10 differential GNSS, in real-time kinematic positioning (RTK) mode, to absolute positions with sub-centimetre precision, measured in WGS 84/UTM zone 33N (EPSG:32633) coordinates. Our survey workflow followed the UAV Structure from Motion (SfM) survey assembly as detailed by Smith and others (2016) and James and others (2017). We collected UAV images with a DJI Mavic 2 Pro drone (Figures S2, S3). We conducted multiple UAV flights, covering Hammarmossen, flown at an elevation of 120 m in calm and sunny conditions. The UAV camera was set with an automatic timer to capture images every 2 s, which provided the best image quality based on elevation and speed, with a sufficient level of overlap between images to enable subsequent photogrammetric analysis (see below). We captured a total of 1806 images at both oblique and nadir angles to aid with the photogrammetric reconstruction, providing a ground resolution of 2.98 cm/pixel.

We processed the UAV imagery using the commercially available software package Agisoft Metashape Version 1.8.3. We loaded all UAV imagery into Agisoft and discarded images with an image quality score of < 0.5, retaining 1663 images. First, we undertook an initial alignment using the 'high' accuracy setting, an optimum option based on the survey size and images (James and others 2017), whereby the software builds a sparse point cloud of several hundred thousand points. We georeferenced the model to the recorded GCP ground survey data, by identifying the GCPs within each image in which they were visible. Doing so enhances spatial accuracy and 3D model geometry (James and others 2017; Rossini and others 2018). Next we conducted a bundle adjustment, whereby the camera alignment is refined by minimising nonlinear deformations and georeferencing errors, with the final XY error $\pm$ 0.06 m. We then performed dense matching using the established survey geometry and camera models to build the final point cloud, made up of 10,086,701 points. This provided detailed topographic data and allowed us to generate a digital elevation model (DEM). As a last step, we generated a very-high-resolution, true-colour orthomosaic, using the DEM and input images as the data source. We exported the orthomosaic at a spatial resolution of 0.05 m for further analysis.

Historical Aerial Photography

We obtained a number of historical black-and-white (timestamp dates 29/04/1961, 17/06/1973, 07/05/2000) and true-colour (red, green, blue; timestamp dates 16/07/2007, 27/06/2010, 23/07/2014, 04/06/2018) aerial images of Hammarmossen, to determine multi-decadal changes in the dynamics of the concentric pools. These historical aerial photographs were provided by Lantmäteriet (the Swedish Land Survey). The pre-1980 images are available as open data from the Lantmäteriet website under the EU Inspire open data policy; later images were available to us as open data under a research licence. All images were available at 0.5 m resolution, apart from the 2000 imagery, which has 1 m resolution. Uncertainties related to aerial images cannot be eliminated entirely due to the absence of field validation from the date of image acquisition; however, we performed a visual appraisal and checked each image for alignment of features within and outside of the Hammarmossen boundary. Where misalignment in static features (for example, electrical pylon towers) was apparent, we made a manual adjustment in QGIS 3.24 (Tisler) to ensure the images were finely co-registered. Because our analysis seeks to distinguish open water from the terrestrial peat surface, rather

than to identify more subtle vegetation gradients or land cover classes, the features of interest, peatland pools, were just as distinct in the black-and-white imagery as in the true-colour imagery.

Photogrammetry and Image Analysis

We performed an object-based image analysis (OBIA) on the UAV and historical aerial photography, using segmentation techniques to identify homogeneous areas. The aim of image segmentation is to delineate objects that represent real-world geographical or ecological features (Shepherd and others 2019; Huang and others 2020), in this instance peatland pools. By grouping together spectrally similar neighbouring pixels based on spectral and geometric properties, it is possible to identify spatiotemporal changes between successive images (Torres-Sánchez and others 2015; Teodoro and Araujo 2016). Our use of OBIA takes advantage of the spatially contiguous nature of landscape features. In order to generate additional image features for the historical and UAV orthomosaic imagery, we used RSGISLib (Bunting and others 2014) to derive whiteness and brightness single-band outputs. Whiteness is a measure of how closely a surface matches the properties of an ideal reflecting diffuser. After experimentation with a number of segmentation algorithms, we applied the mean shift algorithm in ArcGIS Pro 2.9. This algorithm uses a moving window to group image pixels iteratively into a segment characterised by spectrally homogenous attributes (Comanicu and Meer 2002). We used a visual appraisal to determine the optimal set of parameters for the entire time series, combined with an over-segmentation approach, whereby an object may be represented by one or more polygons (Liu and Xia 2010; Watson and others 2016). Outputs from the algorithm are in a raster format, which were vectorised and exported for analysis.

Subsequently, we used QGIS 3.24 (Tisler) for GIS steps. We populated the attribute table for each year of analysis with statistics for the original imagery: the mean, median, standard deviation and variance in each object for the corresponding channels. We identified waterbodies and pools both manually and using thresholding of the attribute table after identifying suitable parameters. We edited polygons where required, for example, in areas of shadow, due to confusion in the OBIA process; however, this was minimal per imagery year. We then dissolved the final pool boundaries and used the single-part to multi-part tool to produce a final waterbody output. We derived area (m^2) and shape characteristics for each pool.

We developed a pool inheritance methodology and workflow to explore spatiotemporal changes in individual waterbodies across the study site. Initially, we assigned a unique, sequentially numbered identifier to each waterbody identified in the most recent imagery (our UAV survey in 2022). Then, we applied a spatial join attributes by location, working back through the time series, such that each waterbody had a unique identifier that was consistent through time. Where a waterbody split into two or more discrete waterbodies, each part was given an additional ‘a’ and ‘b’, etc., suffix. In instances where pools merged, the identifier was inherited by the pool with the largest area. In instances where there was a pool present in older imagery that was not present in 2022, we assigned it the year and a sequential number, for example 2018_01, 2014_01 and so forth. Once each year’s waterbodies had a unique identifier, we loaded them into a Jupyter Notebook and read them as individual Pandas dataframes (McKinney 2010; Reback and others 2021) before performing an outer join to merge the years into a single dataset based on the unique identifier.

Next, we calculated absolute changes in pool areas (m^2) between years and assigned these to the corresponding time periods. Four values were assigned to a new column per time period, thereby characterising the dynamics of the pool during that period. When compared to the antecedent area, four modes of change are possible: **initiation** represents the appearance of a newly formed waterbody, **growth** represents an increase in size, **shrinkage** represents a decrease in size and **expiration** represents where the waterbody has disappeared from one timestamp to the next. These values were assigned based on conditional statements on the individual waterbodies areas. For example, if waterbody ‘1’ had a positive increase in area between 1961 and 1973, time period one for the waterbody was assigned ‘Growth’. The area changes for each time period were then converted to a rate of change per year. Our final data set comprised spatiotemporally discriminated waterbodies with descriptors of areal size within a given time period, absolute changes in area and the type of change that has occurred.

Secondary Data Sources

For illustrative purposes (Figure 1C), we obtained airborne Light Detection and Ranging (LiDAR) data distributed by Lantmäteriet under their open re-

search data programme. The raw LiDAR dataset was provided in LAZ format, this was converted to LAS using LAStools (rapidlasso 2022) with this then processed into a digital terrain model (DTM) and digital surface model (DSM) at a spatial resolution of 1 m. Data on daily temperature and precipitation were obtained in CSV format from the Swedish Meteorological and Hydrological Institute (SMHI). The dataset is from the SMHI Precipitation Temperature Hydrological Agency's Water Model (Precipitation Temperature Hydrologiska Byåns Vattenmodell, PTHBV) database, where daily meteorological station data have been interpolated to a nationwide grid with a resolution of 4 × 4 km (Olsson and others 2013). We used these daily data to calculate monthly precipitation, monthly mean temperature and the departures of monthly precipitation and temperature from the climatological means. We also calculated 12-month trailing mean temperature and precipitation values, to reduce the impact of temporary fluctuations and to obtain a more stable representation of the underlying climate. We calculated the annual growing degree-days above + 5 °C (GDD_5), which we define as the time integral of monthly air temperatures above 5 °C (Nordström and others 2022).

Results

Peatland-Scale Changes in Open-Water Area

Between 1961 and 2022, total pool area at Hammarmossen decreased (Figure 3A). Individual pools commonly lost open-water area and infilled (Figure 3A, 4, S8). Total pool area was greatest in 1961, at 228,131 m^2 (n = 449 individual pools), and by 2022, this had declined to 167,096 m^2 (n = 429), representing a decrease of 26.8% compared to the 1961 open-water area and a net loss of 20 individual pools. This is equivalent to an annual loss of pool area of 1001 m^2 y^{-1}.

The loss of open-water area during our study period began slowly and then accelerated in later decades. During the 12-year period between 1961 and 1973, at the beginning of the time series, there was only a small decrease in open-water pools of 0.9%, to an area of 226,051 m^2 (n = 441). This is a decrease of 2080 m^2, equivalent to a net rate of change of − 173 m^2 y^{-1} (Figure 5), which contrasts with the much more rapid change observed over the 61-year period as a whole. By 2000, total pool area had declined to 203,712 m^2 (n = 451), representing a 10.7% decrease in total pool area since 1961. Between 1973 and 2000 the equivalent net rate of change was − 827 m^2 y^{-1}. During the 7-year period between 2000 and 2007, there was a decrease in open-water pools to an area of 191,736 m^2 (n = 410), a 5.9% decrease in total pool and a net rate of change of − 1711 m^2 y^{-1}. The subsequent 3-year period had a further decrease in open-water pools to an area 185,488 m^2 (n = 422), equivalent to a 3.3% decrease in total pool area but a net rate of change of − 2083 m^2 y^{-1} (Figures 3A, 5).

The greatest net rate of change in total pool area occurred between 2010 and 2014 (− 2964 m^2 y^{-1}, Figure 5), representing an overall decrease of 6.4% over the 4-year period. Areas changed from 185,488 m^2 (n = 422) to 173,631 m^2 (n = 405, Figure 3A), respectively. Net loss accelerated periodically and steadily until 2014, when the net change slowed in the subsequent time periods (Figure 5). The net change rate for 2014–2018 (− 604 m^2 y^{-1}) was the slowest rate of change since 1961–1973. The overall pool area change between 2014 and 2018 was a decrease of 1.4%. The most recent period showed an areal decrease of 2.4%, from 171,214 m^2 (n = 414) in 2018 to an area of 167,096 m^2 (n = 429) in 2022, a net change of − 1029 m^2 y^{-1}.

The monotonic loss open-water area at Hammarmossen occurred at the same time as, and may be partly explained by, some pronounced changes in climate (Figure 3B, C, D). The annual time integral of monthly air temperatures above 5 °C (GDD_5) and 12-month mean temperature both increase linearly during the 61-year study period, while total precipitation remained relatively stable (Figure 3B, C, D). The observed period during which pool area underwent the most rapid net loss, 2010–2014 (− 2964 m^2 y^{-1}, Figure 5), coincided with a strong fluctuation in 12-month mean temperature, which rebounded from 3.14 to 7.02 °C (Figure 3C). This increase in 12-month trailing mean temperature coincides with a period of warming winters, as measured by the time integral of months below 0 °C (Figure S7). The highest 12-month trailing precipitation values were recorded in 2001 (Figure 3D), although the time series is noisy. Between 2010 and 2014, GDD_5 was 1380 °C days, with a peak of 1527 °C days recorded in 2011. The highest annual GDD_5 values occurred in 2018, which experienced 1753 °C days (Figure 3B).

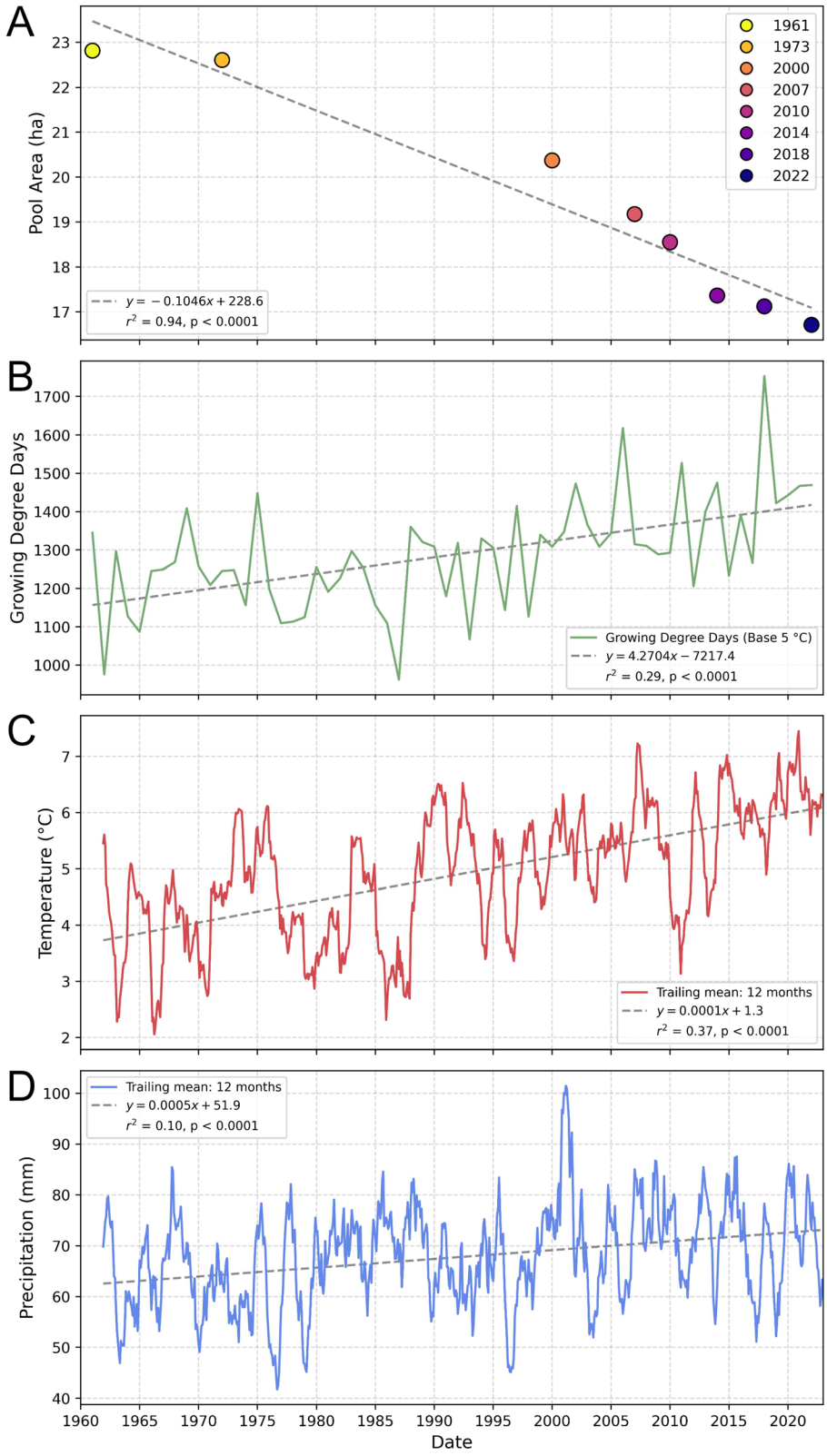

Figure 3. Observed change in total annual pool area from 1961 to 2022 (**A**), with Growing Degree Days (base 5 °C) (**B**), 12-month trailing mean temperature (**C**) and precipitation values (**D**) for the same period, displayed alongside linear regressions. Colours (**A**) match those displayed in Figures 4, 7 and S8.

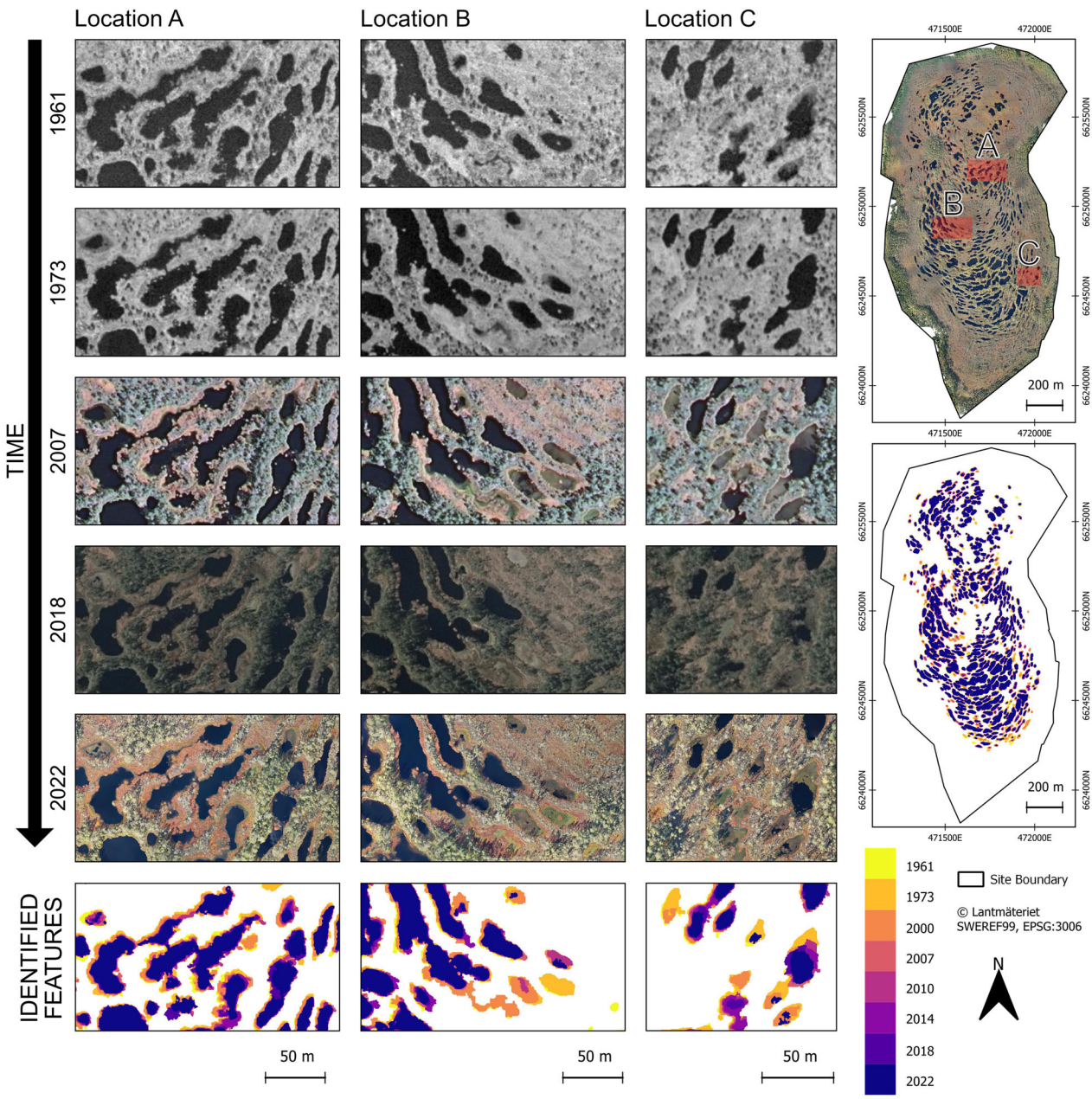

Figure 4. Time series showing examples of aerial photographs from three selected locations around the site (upper right inset). Bottom panels show change in areas classified as pools. Central right inset shown in Figure S8.

Pool-Scale Hydrological Changes in Open-Water Area

In addition to the peatland-scale analysis described above, we explored pool-scale spatiotemporal changes at the site (Figure 4). For each period between successive aerial images, we calculated the total areal changes in pool area accounted for by each mode of change (initiation, growth, shrinkage, expiration), alongside normalised annual area net change, for individual pools (Figure 5). The loss of pool area observed across the site (Figure 3) appears to be driven predominantly by overgrowth, infilling and encroachment of pools by aquatic mosses, rather than pool drainage (Figure 4). This phenomenon is aptly demonstrated by monitoring example pools, such as those labelled as Locations B and C in Figure 4, where the infilling and encroachment of pools with aquatic mosses and peat can be clearly observed between 1961 and 2022. The shrinking of inter-pool channels is also evident in Location A during the same time period,

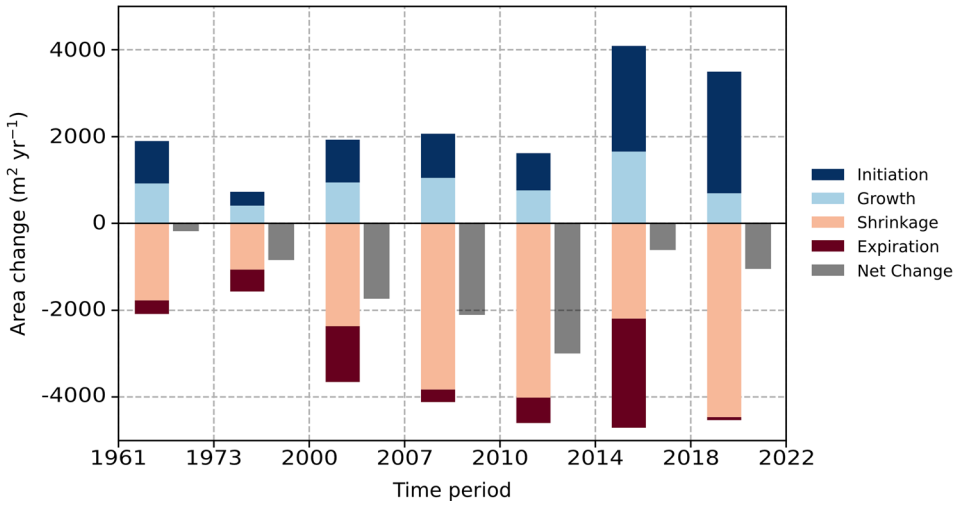

Figure 5. Summary of modes and rates of area changes in open-water pools between 1961 and 2022, alongside net change (m^2 y^{-1}), where each bar represents the period between observations.

as a narrowing and then disappearance of inter-pool channels which again become colonised by mosses. Field observations suggest that infilling from pool margins is by submerged and floating *Sphagnum cuspidatum*, followed by quaking carpets of *S. magellanicum* agg. The changes observed in this location correspond to the area loss between time periods being dominated by pool shrinking, rather than expiration (Figure 5). For most time periods, pool shrinkage is the most prominent mode of change, resulting in an approximately linear rate of areal loss (Figures 3A, 5). For 2014–2018, expiration is also particularly prominent (Figure 5).

In contrast to the linear, monotonic decrease in total pool area at the site scale, individual pools exhibited complex changes in topology and area during the study period. For example, some open-water pools in Figure 4, Location B, noticeably grew between 1961 and 1973. The dynamic, heterogeneous nature of the site is exemplified by levels of growth between each time period (Figure 5). Whilst the overall change between 1961 and 1973 was a 0.9% decrease in open-water pool area (Sect. ''Peatland-scale Changes in Open-Water Area''), the growth and initiation of pools accounted for 927 m^2 y^{-1} and 979 m^2 y^{-1}, respectively (Figure 5). Shrinkage and expiration of open-water pools for 1961–1973 were -1765 m^2 y^{-1} and − 313 m^2 y^{-1}, resulting in a net change of − 173 m^2 y^{-1} (Figure 5). The two pools in the east of Figure 4, Location B, decreased in size across the observed time period, disappearing by 2018, with only a partial residual open-water pool present in 2007. Obvious colour differences can be seen between vegetation on established lawns and the greenish parts (indicating carpets of species such as *Sphagnum cuspidatum*) in recently infilled pools in this area (Figure 4, Location B, 2022). A pair of connected pools is visible in Figure 4, Location C, for the years 1961 through 2007, but by 2018 this had become two separate pools after the narrow, inter-pool channel had overgrown. Furthermore, the two separate pools continued to shrink in size after this time period. The main mode of change between 2018 and 2022 is shrinking, representing a change of − 4460 m^2 y^{-1}. Whilst this area was shrinking, the pool located in the south–central area of Figure 4, Location C, shrank from 1961 to 2018, and by 2022, it had infilled completely. Of the modes of change in pool area during the 61-year time period, pool shrinkage was the dominant process, indicating the loss of pool area due to overgrowth and encroachment by aquatic mosses (for example, *Sphagnum cuspidatum*). Nonetheless, all modes of change (initiation, growth, shrinkage, expiration) were evident at different times and locations, including the complete expiration of pools through overgrowth by moss (for example, Figure S4).

The largest areal loss of open-water through pool expiration occurred between 2014 and 2018, when a greater area of pools expired than shrunk (− 2512 m^2 y^{-1} against − 2186 m^2 y^{-1}). This time period was particularly dynamic, with a large number of initiations observed as well, resulting in the smallest annual net change (Figure 5). From 2014 onwards there is a trend towards increased dynamism; there is a degree of turnover for open-water pools accounting for lower negative net change values (Figure 5). The rate of areal change

per year (% y^{-1}) is driven by smaller pools, shrinking and growing (Figure 6A). Larger pools underwent more subtle rates of areal change on a percentage basis, whereas similar linear rates of growth or shrinkage represent greater percentage areal changes in smaller pools. This is exemplified by comparing the median sizes of pools which expired (ranging from 18 to 136 m^2, Figure 6B), to the median sizes of all pools that existed at the start of each time period (ranging from 196 to 272 m^2, Figure 6B). In short, it is predominately smaller pools that are being infilled across the site (Figure 6B).

Discussion

Peatland-Scale Loss in Open-Water Area

Our analysis of six decades of aerial photography shows a large and rapid decrease in pool area from 228,131 m^2 (n = 449 individual pools) in 1961 to 167,096 m^2 (n = 429) in 2022, equivalent to a loss of just over a quarter of the original pool area (26.8%). This equates to an average annual rate of loss of pool area of 1001 m^2 y^{-1}, indicating that the site is changing rapidly. If this trend of pool loss is to continue for many more decades, then this ico-

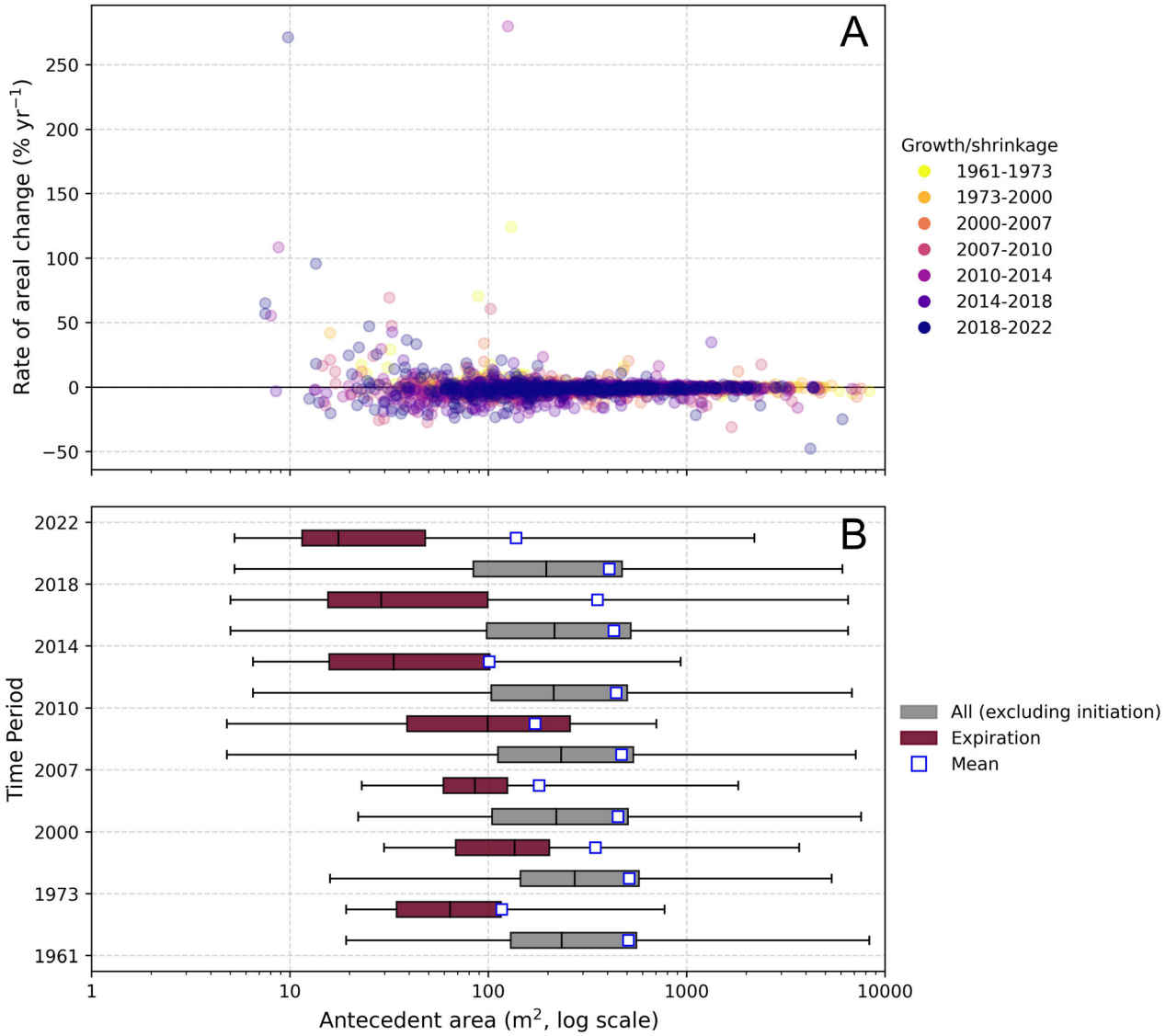

Figure 6. Spatiotemporal variation in open-water pools between 1961 and 2022, showing (**A**) rate of areal change against antecedent area and (**B**) the distribution of pool sizes that expire in each time step (dark red fill), compared to all pools excluded those that initiate in each step (grey fill). Box hinges represent the 25th and 75th percentiles; the central bar indicates the 50th percentile and whiskers show 5th and 95th percentiles.

nic peatland site may be in danger of losing its characteristic surface patterning.

A number of previous studies have reported rapid recent decreases in open-water area and/or in wet terrestrial habitat areas (for example, hollows), across a range of types of northern peatlands (Granlund and others 2022; Kolari and others 2022; Steenvoorden and others 2022). Kolari and others (2022) explored the fen–bog transition in a boreal aapa mire, observing a 46% decrease in flark area across their study site between 1947 and 2019, equivalent to a lateral expansion of *Sphagnum* cover at a rate of 30 cm y^{-1}. A similar study by Granlund and others (2022) explored middle and northern boreal aapa mires, observing decreases in flark areas between 16 and 63% in 47–74 years, with an average lateral expansion rate of 0.77 m y^{-1} as detected by aerial photograph analysis and 0.71 m y^{-1} as detected from an analysis of a transect of peat cores. We acknowledge that factors driving fen–bog transitions on aapa mires may differ from those in raised bogs, such as our study site; however, the similarly rapid loss of open-water area is striking.

Drivers and Mechanisms

The development and maintenance of peatland pools have been discussed in numerous previous studies (for example, Foster and others 1983, 1988; Foster and Wright 1990; Belyea and Lancaster 2002; Belyea and Baird 2006; Eppinga and others 2009a), and the infilling of open water by *Sphagnum* carpets is thought to form part of hydroseral succession (Gorham 1957; Kuhry and others 1993; Kolari and others 2022). Our observations suggest the multi-decadal loss of open-water area at Hammarmossen has occurred primarily through infilling and encroachment (Figures 4, 5, 7), whereby a floating mat forms consisting of mosses, vascular plants and dead organic material, initiated at the pool bottom, the shoreline or from free-floating vegetation mats (Temmink and others 2021). As outlined by Foster and Wright (1990), sufficient vertical accretion of peat allows micro-scale topographic differences to develop, in turn causing water to collect in low-lying areas to form pools. Plant growth within the pool can be restricted due to a lack of oxygen, whilst continued plant growth and litter formation on adjacent ridges can increase the height of the ridge, leading to a deepening of the pool (Sjörs 1990; Belyea and Clymo 2001; Belyea 2007). Older, deeper pools are found at the centre of Hammarmossen, while marginal pools are generally younger and shallower (Foster and Wright 1990). It has been noted that larger and deeper pools may ultimately fill up with gyttja, allowing the surface to support the growth of mosses and sedges (Foster and Wright 1990; Ammann and others 2013). However, the net loss of pool area during our study period (Figure 5) is primarily attributable to the shrinkage and expiration of smaller pools (Figure 6B). From the work conducted by Foster and Wright (1990) at our study site, it can be inferred that these smaller pools are typically younger and shallower than the larger, more stable pools. It may be that shallower water leads to a more rapid expansion of *Sphagnum* if hydrological conditions allow (Granlund and others 2022).

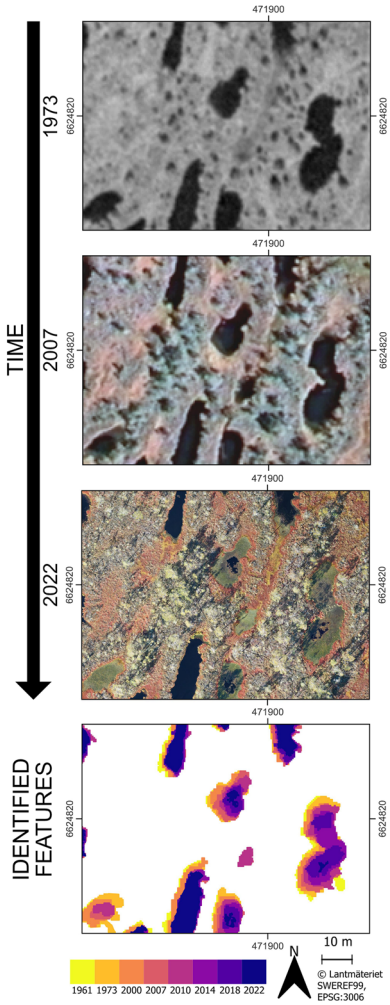

Figure 7. Time series showing examples of aerial photographs for a select location, illustrating spatiotemporal variation in shrinkage/expiration of identified open-water areas.

It has been proposed that as peatlands develop, the proportional cover of pools tends to increase and that of terrestrial habitats tends to decrease, through autogenic mechanisms (Foster and Fritz 1987; Foster and others 1988; Karofeld 2004; Belyea 2007). Smaller pools can coalesce and enlarge through bog development (Foster and Wright 1990). Using a theoretical model of patterned peatland initiation and development, Belyea (2007) noted that once pools contain surface water throughout the year with no continuous vegetation cover, reversal back to a terrestrial state becomes highly unlikely unless catastrophic drainage occurs. For our study area, open-water pools appear not to be stable in the way suggested, as shown by pool shrinkage and expiration occurring over the study period (Figures 5, 6), with vegetation cover initiated by the invasion of floating and even submerged *Sphagnum* (for example, Figures S4, S5). Discussions on mechanisms have focused on the initiation and maintenance of pools. For infilling, the likely scenario is that *Sphagnum cuspidatum* invades as floating and submerged horizontally growing shoots. As the *S. cuspidatum* cover becomes denser, increased buoyancy allows it to shift to upright growth. This provides a habitat for *S. magellanicum* agg. and other erect-growing species, and also for vascular plants. Their rhizomes then fortify and stabilise the nascent carpet. How such an infilling scenario is controlled by water level, climate and biological interactions is however largely unknown and requires further investigation. If small pools do merge and enlarge, as suggested by Foster and Wright (1990), our results imply that this is currently happening more slowly than the observed infilling.

Canadian peatlands with characteristics similar to Hammarmossen have been explored (Arsenault and others 2019; Robitaille and others 2021), with Grande plée Bleau being a notable ombrotrophic example (~ 650 open-water pools, Arsenault and others 2019). It was found that open-water pools seem to play a role in dictating the hydrological gradients of peatland sites, and are thus important for nutrient movement (Arsenault and others 2019, 2022). Water-level fluctuations can also impact vegetation health within peatland environments (Granath and others 2010; Waddington and others 2015; Zhong and others 2020; Kolari and others 2021; Magnan and others 2022). We do not possess long-term hydrological monitoring data for the site, and so we cannot strictly rule out changes in the site's water budget as a cause of pool loss. Nonetheless, the loss of pool area appears to be due to overgrowth of open-water surfaces by *Sphagnum* carpets, leading to the formation of quaking mire surfaces in some examples (Byun and others 2022; Granlund and others 2022; Kolari and others 2022; Zhang and others 2022b), rather than evaporative drying or hydrotopographic drainage.

Hammarmossen has experienced changes in climate (Figure 3B, 3C) during the study period, which may be responsible for the pronounced changes in open-water area. In particular, longer, warmer growing seasons (Figure 3B) are likely to have stimulated moss and sedge growth in the pools. In some cases, raised bog vegetation can result from autogenic succession, in which terrestrialisation occurs via the infilling of a water body with organic and inorganic material over timescales of centuries to millennia (Foster and Wright 1990; Ruppel and others 2013). The progress of a peatland along this development pathway may be accelerated by allogenic factors, including climatic warming (Hughes and Barber 2004; Sim and others 2019; Swindles and others 2019; Kolari and others 2021; Kolari and others 2022; Sallinen and others 2023). For example, Kolari and others (2021) observed an increase in *Sphagnum* mosses that coincided with a 20-year period of significant warming, encompassing an area of rich fen in eastern Finland. In Canada, shifts towards drier bogs have been observed, likely in part due to substantial warming where an increase in GDDs was noted with precipitation remaining stable (Magnan and others 2018, 2022). Others have noted pool infilling in line with an increase in temperature and GDD_5 over a similar period to our study, 1950–2017, with paleo-records from boreal sites (Robitaille and others 2021), indicating that longer and warmer growing seasons are at least partially contributing to these observed changes. Warming observed in Hammarmossen has been of similar magnitude as in the studies where the increase in moss and sedge productivity has been connected to climatic warming (Loisel and others 2012; Bengtsson and others 2021; Kolari and others 2021; Robitaille and others 2021; Kolari and others 2022; Magnan and others 2022).

Despite the consistent, monotonic net loss of open-water pool area during the study period, each time period also exhibits growth and initiation of individual pools (Figure 5, 6). It may be tempting to attribute these changes, at least in part, to the timing of image acquisition each year, given likely phenological changes in bog pools, particularly given that 1961 has the greatest pool area and the earliest acquisition date. Dates of image acquisition in subsequent years varied randomly throughout the growing season, yet the time series as a whole

still indicates monotonic decrease in open-water pool area. Changes observed had a clear temporal trend, similar to that reported by Kolari and others (2022) and Granlund and others (2022). As such, we are confident that any phenological artefact is not so great as to have led to the false identification of a long-term drying trend. Furthermore, Arsenault and others (2019) found that even during periods of dry weather, when the water table drops rapidly within the peat due to evapotranspiration, water level in pools remained more stable. Our site is an ombrotrophic peatland in which nutrients and moisture are derived solely from atmospheric sources, with surface patterning influenced by patterns of water and/or nutrient flow (Belyea 2007). The initiation of any new pools through the autogenic mechanisms outlined by Foster and Wright (1990) are apparently being outweighed by other factors, driving a net loss of pool area and number through shrinkage and expiration during our study period. Climatic warming seems the most likely driver for this loss of pool area (Figure 3), although we cannot rule out the possibility of autogenic mechanisms for pool loss.

Conclusions

We combined a multi-decadal time series of aerial images with a pool inheritance methodology to explore changes in pool characteristics on a patterned raised bog in boreal Sweden. Our analysis indicates that the site has changed rapidly, with pools commonly being overgrown by encroaching *Sphagnum* mats. Between 1961 and 2022, total pool area decreased by 26.8% at an average net rate of 1001 m^2 y^{-1}. Similar loss of open-water area has recently been reported in other sites in boreal peatlands and elsewhere, and we suspect rapid recent changes in our study site are being driven by ongoing climatic warming that is accelerating moss growth and infilling. Previous work at our study site hypothesised that smaller pools tend to merge and enlarge through autogenic mechanisms; if this is the case, then it is happening more slowly than pool infilling and *Sphagnum* encroachment. The rapid overgrowth of pools at our site, and elsewhere, also disagrees with existing theories that pools are highly stable once formed. The rapid changes at our study site indicate the importance of monitoring microform dynamics, a task to which repeat UAV surveys are well suited. Although climate change seems a likely driver for pool overgrowth, the precise mechanism is largely unknown and warrants further investigation. Doing so may provide an improved understanding of impacts upon peatland carbon budgets, habitat provision and water resources in future decades.

Acknowledgements

This work was supported by the Leeds-York-Hull Natural Environment Research Council (NERC) Doctoral Training Partnership (DTP) Panorama under grant NE/S007458/1, awarded to D.W.C. We are grateful to the Örebro County board for granting the relevant authorisation for our survey.

Data Availability

The historical aerial photography and LiDAR data were obtained from Lantmäteriet under their open research programme (https://www.lantmateriet.se/en/geodata/geodata-products/open-data/). Meteorological data were obtained from the Swedish Meteorological and Hydrological Institute's Precipitation Temperature Hydrologiska Byåns Vattenmodell (https://www.smhi.se/data/ladda-ner-data/griddade-nederbord-och-temperaturdata-pthbv). Generated outputs are available from https://doi.org/10.5281/zenodo.8189607.

References

Almendinger JE, Leete JH. 1998. Regional and local hydrogeology of calcareous fens in the Minnesota River basin, USA. Wetlands 18:184–202.

Almquist-Jacobson H, Foster DR. 1995. Toward an integrated model for raised-bog development: theory and field evidence. Ecology 76:2503–2516.

Almquist-Jacobson HA. 1994. Interaction of Holocene climate, water balance, vegetation, fire, and cultural land-use in the Swedish Borderland.

Ammann B, van Leeuwen JFN, van der Knaap WO, Colombaroli D, Tinner W, Wright HE, Stefanova V. 2013. The role of peat decomposition in patterned mires: a case study from the central Swiss Alps. Preslia 85:317–332.

Arsenault J, Talbot J, Brown LE, Holden J, Martinez-Cruz K, Sepulveda-Jauregui A, Swindles GT, Wauthy M, Lapierre J-F. 2022. Biogeochemical distinctiveness of peatland ponds, thermokarst waterbodies, and lakes. Geophys Res Lett 49:e2021GL097492.

Arsenault J, Talbot J, Moore TR, Beauvais M-P, Franssen J, Roulet NT. 2019. The spatial heterogeneity of vegetation, hydrology and water chemistry in a peatland with open-water pools. Ecosystems 22:1352–1367.

Beadle JM, Brown LE, Holden J. 2015. Biodiversity and ecosystem functioning in natural bog pools and those created by rewetting schemes. Wires Water 2:65–84.

Belyea LR. 2007. Climatic and topographic limits to the abundance of bog pools. Hydrol Process 21:675–687.

Belyea LR, Baird AJ. 2006. Beyond ''the limits to peat bog growth'': cross-scale feedback in peatland development. Ecol Monogr 76:299–322.

Belyea LR, Clymo RS. 2001. Feedback control of the rate of peat formation. Proc R Soc Lond Ser B Biol Sci 268:1315–1321.

Belyea LR, Lancaster J. 2002. Inferring landscape dynamics of bog pools from scaling relationships and spatial patterns. J Ecol 90:223–234.

Bengtsson F, Rydin H, Baltzer JL, Bragazza L, Bu Z-J, Caporn SJM, Dorrepaal E, Flatberg KI, Galanina O, Gałka M, Ganeva A, Goia I, Goncharova N, Hájek M, Haraguchi A, Harris LI, Humphreys E, Jiroušek M, Kajukało K, Karofeld E, Koronatova NG, Kosykh NP, Laine AM, Lamentowicz M, Lapshina E, Limpens J, Linkosalmi M, Ma J-Z, Mauritz M, Mitchell EAD, Munir TM, Natali SM, Natcheva R, Payne RJ, Philippov DA, Rice SK, Robinson S, Robroek BJM, Rochefort L, Singer D, Stenøien HK, Tuittila E-S, Vellak K, Waddington JM, Granath G. 2021. Environmental drivers of *Sphagnum* growth in peatlands across the Holarctic region. J Ecol 109:417–431.

Bunting P, Clewley D, Lucas RM, Gillingham S. 2014. The remote sensing and GIS software library (RSGISLib). Comput Geosci 62:216–226.

Byun E, Cowling SA, Finkelstein SA. 2022. Holocene regional climate change and formation of southern Ontario's largest swamp inferred from a kettle-lake pollen record. Quat Res 106:56–74.

Chapman PJ, Moody CS, Turner TE, McKenzie R, Dinsmore KJ, Baird AJ, Billett MF, Andersen R, Leith F, Holden J. 2022. Carbon concentrations in natural and restoration pools in blanket peatlands. Hydrol Process 36:e14520.

Comaniciu D, Meer P. 2002. Mean shift: a robust approach toward feature space analysis. IEEE Trans Pattern Anal Mach Intell 24:603–619.

Couwenberg J, Joosten H. 2005. Self-organization in raised bog patterning: the origin of microtope zonation and mesotope diversity. J Ecol 93:1238–1248.

Eppinga MB, de Ruiter PC, Wassen MJ, Rietkerk M. 2009a. Nutrients and hydrology indicate the driving mechanisms of peatland surface patterning. Am Nat 173:803–818.

Eppinga MB, Rietkerk M, Wassen MJ, De Ruiter PC. 2009b. Linking habitat modification to catastrophic shifts and vegetation patterns in bogs. Plant Ecol 200:53–68.

Foster DR, Fritz SC. 1987. Mire development, pool formation and landscape processes on patterned fens in Dalarna, central Sweden. J Ecol 75:409–437.

Foster DR, King GA, Glaser PH, Wright HE. 1983. Origin of string patterns in boreal peatlands. Nature 306:256–258.

Foster DR, Wright HE, Thelaus M, King GA. 1988. Bog development and landform dynamics in central Sweden and southeastern Labrador, Canada. J Ecol 76:1164–1185.

Foster DR, Wright HE Jr. 1990. Role of ecosystem development and climate change in bog formation in central Sweden. Ecology 71:450–463.

Gorham E. 1957. The development of peat lands. Q Rev Biol 32:145–166.

Gorham E. 1991. Northern peatlands: role in the carbon cycle and probable responses to climatic warming. Ecol Appl 1:182–195.

Granath G, Strengbom J, Rydin H. 2010. Rapid ecosystem shifts in peatlands: linking plant physiology and succession. Ecology 91:3047–3056.

Granlund L, Vesakoski V, Sallinen A, Kolari THM, Wolff F, Tahvanainen T. 2022. Recent Lateral Expansion of *Sphagnum* Bogs over Central Fen Areas of Boreal Aapa Mire Complexes. Ecosystems 25:1455–1475.

Huang H, Lan Y, Yang A, Zhang Y, Wen S, Deng J. 2020. Deep learning versus object-based image analysis (OBIA) in weed mapping of UAV imagery. Int J Remote Sens 41:3446–3479.

Hughes PDM, Barber KE. 2004. Contrasting pathways to ombrotrophy in three raised bogs from Ireland and Cumbria, England. The Holocene 14:65–77.

James MR, Robson S, Smith MW. 2017. 3-D uncertainty-based topographic change detection with structure-from-motion photogrammetry: precision maps for ground control and directly georeferenced surveys. Earth Surf Process Landf 42:1769–1788.

Karofeld E. 2004. Mud-bottom hollows: exceptional features in carbon-accumulating bogs? The Holocene 14:119–124.

Kolari THM, Korpelainen P, Kumpula T, Tahvanainen T. 2021. Accelerated vegetation succession but no hydrological change in a boreal fen during 20 years of recent climate change. Ecol Evol 11:7602–7621.

Kolari THM, Sallinen A, Wolff F, Kumpula T, Tolonen K, Tahvanainen T. 2022. Ongoing fen-bog transition in a boreal aapa mire inferred from repeated field sampling, aerial images, and Landsat data. Ecosystems 25:1166–1188.

Kuhry P, Nicholson BJ, Gignac LD, Vitt DH, Bayley SE. 1993. Development of *Sphagnum*-dominated peatlands in boreal continental Canada. Can J Bot 71:10–22.

Lindsay R. 2010. Peatlands and carbon: a critical synthesis to inform policy development in peatland conservation and restoration in the context of climate change. IUCN UK Peatlands

Liu D, Xia F. 2010. Assessing object-based classification: advantages and limitations. Remote Sens Lett 1:187–194.

Loisel J, van Bellen S, Pelletier L, Talbot J, Hugelius G, Karran D, Yu Z, Nichols J, Holmquist J. 2017. Insights and issues with estimating northern peatland carbon stocks and fluxes since the Last Glacial Maximum. Earth-Sci Rev 165:59–80.

Loisel J, Gallego-Sala AV, Amesbury MJ, Magnan G, Anshari G, Beilman DW, Benavides JC, Blewett J, Camill P, Charman DJ,

Chawchai S, Hedgpeth A, Kleinen T, Korhola A, Large D, Mansilla CA, Müller J, van Bellen S, West JB, Yu Z, Bubier JL, Garneau M, Moore T, Sannel ABK, Page S, Väliranta M, Bechtold M, Brovkin V, Cole LES, Chanton JP, Christensen TR, Davies MA, De Vleeschouwer F, Finkelstein SA, Frolking S, Gałka M, Gandois L, Girkin N, Harris LI, Heinemeyer A, Hoyt AM, Jones MC, Joos F, Juutinen S, Kaiser K, Lacourse T, Lamentowicz M, Larmola T, Leifeld J, Lohila A, Milner AM, Minkkinen K, Moss P, Naafs BDA, Nichols J, O'Donnell J, Payne R, Philben M, Piilo S, Quillet A, Ratnayake AS, Roland TP, Sjögersten S, Sonnentag O, Swindles GT, Swinnen W, Talbot J, Treat C, Valach AC, Wu J. 2021. Expert assessment of future vulnerability of the global peatland carbon sink. Nat Clim Chang 11:70–77.

Loisel J, Gallego-Sala AV, Yu Z. 2012. Global-scale pattern of peatland *Sphagnum* growth driven by photosynthetically active radiation and growing season length. Biogeosciences 9:2737–2746.

Magnan G, van Bellen S, Davies L, Froese D, Garneau M, Mullan-Boudreau G, Zaccone C, Shotyk W. 2018. Impact of the Little Ice Age cooling and 20th century climate change on peatland vegetation dynamics in central and northern Alberta using a multi-proxy approach and high-resolution peat chronologies. Quat Sci Rev 185:230–243.

Magnan G, Sanderson NK, Piilo S, Pratte S, Väliranta M, van Bellen S, Zhang H, Garneau M. 2022. Widespread recent ecosystem state shifts in high-latitude peatlands of northeastern Canada and implications for carbon sequestration. Glob Chang Biol 28:1919–1934.

Mantilla I, Flanagan K, Muthanna TM, Blecken G-T, Viklander M. 2023. Variability of green infrastructure performance due to climatic regimes across Sweden. J Environ Manag 326:116354.

McKinney W. 2010. Data structures for statistical computing in Python. In: Proceedings of the 9th Python in Science Conference. pp. 56–61.

Morris PJ, Swindles GT, Valdes PJ, Ivanovic RF, Gregoire LJ, Smith MW, Tarasov L, Haywood AM, Bacon KL. 2018. Global peatland initiation driven by regionally asynchronous warming. Proc Natl Acad Sci 115:4851–4856.

Müller J, Joos F. 2020. Global peatland area and carbon dynamics from the Last Glacial Maximum to the present—a process-based model investigation. Biogeosciences 17:5285–5308.

Müller J, Joos F. 2021. Committed and projected future changes in global peatlands—continued transient model simulations since the Last Glacial Maximum. Biogeosciences 18:3657–3687.

Nordström E, Eckstein RL, Lind L. 2022. Edge effects on decomposition in *Sphagnum* bogs: implications for carbon storage. Ecosphere 13:e4234.

Olsson J, Södling, J, Wetterhall, F. 2013. Högupplösta nederbördsdata för hydrologisk modellering: en förstudie. SMHI

Page SE, Rieley JO, Banks CJ. 2011. Global and regional importance of the tropical peatland carbon pool. Glob Chang Biol 17:798–818.

Pedrotti E, Rydin H, Ingmar T, Hytteborn H, Turunen P, Granath G. 2014. Fine-scale dynamics and community stability in boreal peatlands: revisiting a fen and a bog in Sweden after 50 years. Ecosphere 5:133.

Peel MC, Finlayson BL, McMahon TA. 2007. Updated world map of the Köppen-Geiger climate classification. Hydrol Earth Syst Sci 11:1633–1644.

rapidlasso GmbH 2022. LAStools—efficient LiDAR processing software.

Reback J, McKinney W, jbrockmendel, Bossche JV den, Augspurger T, Cloud P, gfyoung, Hawkins S, Sinhrks, Roeschke M, Klein A, Petersen T, Tratner J, She C, Ayd W, Naveh S, Garcia M, Schendel J, patrick, Hayden A, Saxton D, Jancauskas V, McMaster A, Gorelli M, Battiston P, Seabold S, Dong K, chrisb1, h-vetinari, Hoyer S. 2021. pandas-dev/pandas: Pandas 1.2.2. Zenodo https://zenodo.org/record/4524629.

Robitaille M, Garneau M, van Bellen S, Sanderson NK. 2021. Long-term and recent ecohydrological dynamics of patterned peatlands in north-central Quebec (Canada). The Holocene 31:844–857.

Rossini M, Di Mauro B, Garzonio R, Baccolo G, Cavallini G, Mattavelli M, De Amicis M, Colombo R. 2018. Rapid melting dynamics of an alpine glacier with repeated UAV photogrammetry. Geomorphology 304:159–172.

Ruppel M, Väliranta M, Virtanen T, Korhola A. 2013. Postglacial spatiotemporal peatland initiation and lateral expansion dynamics in North America and northern Europe. The Holocene 23:1596–1606.

Rydin H, Jeglum JK. 2013. The biology of peatlands, 2nd edn. Oxford: Oxford University Press.

Sallinen A, Akanegbu J, Marttila H, Tahvanainen T. 2023. Recent and future hydrological trends of aapa mires across the boreal climate gradient. J Hydrol 617:129022.

Scharlemann JP, Tanner EV, Hiederer R, Kapos V. 2014. Global soil carbon: understanding and managing the largest terrestrial carbon pool. Carbon Manag 5:81–91.

Shepherd JD, Bunting P, Dymond JR. 2019. Operational large-scale segmentation of imagery based on iterative elimination. Remote Sens 11:658.

Sim TG, Swindles GT, Morris PJ, Gałka M, Mullan D, Galloway JM. 2019. Pathways for ecological change in Canadian high arctic wetlands under rapid twentieth century warming. Geophys Res Lett 46:4726–4737.

Sjörs H. 1948. Myvegetation i Bergslagen. Acta Phytogeogr Suec 21:1–299.

Sjörs H. 1990. Divergent successions in mires, a comparative study. Aquil Ser Bot 28:67–77.

SMHI. Climate scenarios. https://www.smhi.se/oceanweb/climate-scenarios-for-the-sea/met/orebro_lan/medelnederbord/rcp45/2011-2040/year/anom Last accessed 27/03/2023

Smith MW, Quincey DJ, Dixon T, Bingham RG, Carrivick JL, Irvine-Fynn TDL, Rippin DM. 2016. Aerodynamic roughness of glacial ice surfaces derived from high-resolution topographic data. J Geophys Res Earth Surf 121:748–766.

Steenvoorden J, Limpens J, Crowley W, Schouten MGC. 2022. There and back again: forty years of change in vegetation patterns in Irish peatlands. Ecol Indic 145:109731.

Swanson DK, Grigal DF. 1988. A simulation model of mire patterning. Oikos 53:309–314.

Swindles GT, Morris PJ, Mullan DJ, Payne RJ, Roland TP, Amesbury MJ, Lamentowicz M, Turner TE, Gallego-Sala A, Sim T, Barr ID, Blaauw M, Blundell A, Chambers FM, Charman DJ, Feurdean A, Galloway JM, Gałka M, Green SM, Kajukało K, Karofeld E, Korhola A, Lamentowicz Ł, Langdon P, Marcisz K, Mauquoy D, Mazei YA, McKeown MM, Mitchell EAD, Novenko E, Plunkett G, Roe HM, Schoning K, Sillasoo Ü, Tsyganov AN, van der Linden M, Väliranta M, Warner B. 2019. Widespread drying of European peatlands in recent centuries. Nat Geosci 12:922–928.

Temmink RJM, Cruijsen PMJM, Smolders AJP, Bouma TJ, Fivash GS, Lengkeek W, Didderen K, Lamers LPM, van der Heide T. 2021. Overcoming establishment thresholds for peat mosses in human-made bog pools. Ecol Appl 31:e02359.

Teodoro AC, Araujo R. 2016. Comparison of performance of object-based image analysis techniques available in open source software (Spring and Orfeo Toolbox/Monteverdi) considering very high spatial resolution data. J Appl Remote Sens 10:016011.

Torres-Sánchez J, López-Granados F, Peña JM. 2015. An automatic object-based method for optimal thresholding in UAV images: application for vegetation detection in herbaceous crops. Comput Electron Agric 114:43–52.

Turner TE, Swindles GT, Roucoux KH. 2014. Late Holocene ecohydrological and carbon dynamics of a UK raised bog: impact of human activity and climate change. Quat Sci Rev 84:65–85.

Waddington JM, Morris PJ, Kettridge N, Granath G, Thompson DK, Moore PA. 2015. Hydrological feedbacks in northern peatlands. Ecohydrology 8:113–127.

Watson CS, Quincey DJ, Carrivick JL, Smith MW. 2016. The dynamics of supraglacial ponds in the Everest region, central Himalaya. Glob Planet Chang 142:14–27.

Xu J, Morris PJ, Liu J, Holden J. 2018a. PEATMAP: refining estimates of global peatland distribution based on a meta-analysis. CATENA 160:134–140.

Xu J, Morris PJ, Liu J, Holden J. 2018b. Hotspots of peatland-derived potable water use identified by global analysis. Nat Sustain 1:246–253.

Zhang H, Väliranta M, Swindles GT, Aquino-López MA, Mullan D, Tan N, Amesbury M, Babeshko KV, Bao K, Bobrov A, Chernyshov V, Davies MA, Diaconu A-C, Feurdean A, Finkelstein SA, Garneau M, Guo Z, Jones MC, Kay M, Klein ES, Lamentowicz M, Magnan G, Marcisz K, Mazei N, Mazei Y, Payne R, Pelletier N, Piilo SR, Pratte S, Roland T, Saldaev D, Shotyk W, Sim TG, Sloan TJ, Słowiński M, Talbot J, Taylor L, Tsyganov AN, Wetterich S, Xing W, Zhao Y. 2022a. Recent climate change has driven divergent hydrological shifts in high-latitude peatlands. Nat Commun 13:4959.

Zhang Y, Gao C, Zhang S, Yang P, Meyers PA, Wang G. 2022b. Significance of different n-alkane biomarker distributions in four same-age peat sequences around the edges of a small maar lake in China. Sci Total Environ 826:154137.

Zhong Y, Jiang M, Middleton BA. 2020. Effects of water level alteration on carbon cycling in peatlands. Ecosyst Health Sustain 6:1806113.